Dependence of the Critical Currents in Superconducting Films on Applied Magnetic Field and Temperature*

J. A. MYDOSH† AND HANS MEISSNER
Department of Physics, Stevens Institute of Technology, Hoboken, New Jersey
(Received 2 July 1965)

Measurements of critical currents i_c were performed on planar and cylindrical films of tin of 650 to 2000 Å thickness. Both pulsed currents (80-nsec duration) and dc currents with stabilizing network were used. Close agreement was obtained for the dc data in the temperature dependence and approximate agreement in the magnitude of the critical current when compared with Bardeen's calculation as long as the stabilizing network was effective. The pulse measurements deviate from theory and from the dc data for temperatures $T/T_c < 0.9$. Oscilloscope pictures of the transitions indicate that this deviation towards lower currents is not caused by usual Joule heating. This and other similar work with pulsed currents and fields would indicate that an entirely new mechanism is responsible for the discrepancy in fast-pulsed critical currents. Critical-current measurements were also taken with the superposition of external magnetic fields H_e. The whole range from the critical current in zero field to the critical field as measured with a current of 100 μA was covered. When the data are plotted as log i_c versus H_e, they form a series of similar curves as the temperature is lowered. If adjusted for a match at $H_e=0$, these curves closely agree with the theoretical predictions of Ginzburg.

I. INTRODUCTION

SUPERCONDUCTIVITY can be destroyed by the application of a magnetic field or a current. For bulk type-I superconductors the current quenching occurs when the magnetic field produced by the current i becomes equal to the critical field H_{cb} of the material.[1] In order to examine the true critical-current quenching, one must use thin films where the critical fields H_c are much larger than in the bulk.

All measurements of the critical current i_c are hampered by two main experimental difficulties: Joule heating in the film at the onset of the normal state and noncompensating geometries causing nonuniform current distributions. It is the aim of the present experiments to eliminate, minimize, or account for these effects. This is accomplished by using both pulsed currents and dc currents with stabilizing network. The pulse measurements are fast enough to suppress most of the heating and yet longer than the delay times found in switching at $i=i_c$. Since heating is minimized, it is possible to use currents large enough to fully restore the normal resistance R_n. The dc method permits the first onset of the normal state to be accurately measured, while a stabilizing network prevents thermal runaway should the heat transfer to the helium bath be unable to keep the temperature of the film constant. In addition, vacuum-deposited films on cylindrical substrates were used to ensure a uniform current distribution. An axial uniform magnetic field can be superposed in order to measure the changes of the critical current with external field H_e.

In the next section we shall give the simple free-energy calculation for critical currents and review the more complicated theories. Also included will be a survey of the previous experiments. Section III will be concerned with a complete description of the present experiment. In Secs. IV and V, we shall present the experimental data and results for the dc and the pulse measurements. The Appendix will contain the theory and the experimental results of films with planar geometry.

II. PREVIOUS WORK

A. Theory

An elementary calculation[2] of the critical current follows from a consideration of the free energy of the superconducting state F_s. To this term let us add the increase in free energy caused by a velocity v_s of the superfluid pairs: $\frac{1}{2}\rho_s v_s^2$, where ρ_s is the density of the superfluid component. For completeness, we can also include the free energy resulting from an external magnetic field: $\frac{1}{2}|\chi|H_e^2$, where χ is the susceptibility. Thus the total free energy becomes

$$(F_s)_{\text{tot}}=F_s+\tfrac{1}{2}\rho_s v_s^2+\tfrac{1}{2}|\chi|H_e^2. \tag{1}$$

The transition to the normal state occurs when $(F_s)_{\text{tot}}=F_n$. Using the free-energy difference between the normal and superconducting states

$$F_n-F_s=H_{cb}^2/8\pi, \tag{2}$$

we obtain

$$H_{cb}^2/8\pi=\tfrac{1}{2}\rho_s v_s^2+\tfrac{1}{2}|\chi|H_e^2. \tag{3}$$

For zero-external field this gives for the critical current density

$$J_c=(e/m)\rho_s v_s=(e/m)(\rho_s/4\pi)^{1/2}H_{cb}. \tag{4}$$

The critical current density can be interpreted in terms of the London penetration depth λ_L by replacing ρ_s with $n_s m$ and using $\lambda_L=(mc^2/4\pi n_s e^2)^{1/2}$, n_s being the

* Based upon a thesis (J. A. M.) submitted to the Department of Physics of the Stevens Institute of Technology in partial fulfillment of the requirements for the Ph.D. degree.

† Present address: Department of Physics, Fordham University, Bronx, New York.

[1] F. B. Silsbee, J. Wash. Acad. Sci. 6, 597 (1916).

[2] J. Bardeen, Rev. Mod. Phys. 34, 667 (1962).

number density of superelectrons. This yields

$$J_c = cH_{cb}/4\pi\lambda_L. \tag{5}$$

If the temperature dependence is included by the approximations

$$H_{cb}(t) = H_{cb}(0)[1-t^2] \tag{6}$$

and

$$\lambda_L(t) = \lambda_L(0)[1-t^4]^{-1/2}, \tag{7}$$

where t is the reduced temperature $t = T/T_c$, then

$$J_c(t) = [cH_{cb}(0)/4\pi\lambda_L(0)](1-t^2)^{3/2}(1+t^2)^{1/2}. \tag{8}$$

However, if we consider the thin film limit, it is customary[3] to replace the London penetration by an effective penetration depth λ, which is equal to

$$\lambda = \lambda_L(\xi_0/\xi(l))^{1/2} = (c^2m^2\xi_0/4\pi\rho_s e^2 l)^{1/2}. \tag{9}$$

The latter term results if the mean free path l is much shorter than the coherence length ξ_0. By performing this replacement at $T=0°$K, substituting the BCS[4] expression for $\xi_0 = \hbar v_f/\pi\Delta(0)$, and using the normal conductivity $\sigma_n = ne^2l/mv_f$ (v_f is the velocity at the Fermi surface and $\Delta(0)$ is one-half the energy gap at 0°K), the critical current density becomes

$$J_c(t) = \frac{H_{cb}(0)}{2}\left(\frac{\sigma_n\Delta(0)}{\hbar}\right)^{1/2}(1-t^2)^{3/2}(1+t^2)^{1/2}. \tag{10}$$

Bardeen[2] has extended the theory by treating the energy gap as a variational parameter to be included in the free energy. In the thin film case he also uses Miller's[5] expression for ρ_s and then finds the gap value which minimizes the free energy. The calculation results in nonanalytic expressions, except for the limiting cases. In the limit of $T \approx 0°$K, the outcome is similar to that of the free-energy calculation with a reduced magnitude of the critical current of about 70%.

Rogers[6] and Parmenter[7] have performed a basic calculation of the critical current from the BCS[4] theory. Electron depairing due to their drift velocities is introduced as the criterion for current quenching.

Another calculation of the critical current was made on the basis of the Ginzburg-Landau[8] (G-L) theory by Ginzburg.[9] For film thicknesses much less than the substrate diameter, the film can be regarded as essentially flat, and the effective wave function Ψ independent of position. This, when combined with the condition $(\kappa d/\lambda)^2 \ll 1$ (κ is a material parameter entering the G-L theory and d is the film thickness), permits the G-L equations to take on a particularly simple form in rectangular coordinates. Also these equations contain the external magnetic field along with the current (both in the longitudinal direction). The critical current density is obtained as the point $d\Psi/dJ = -\infty$ in the implicit solution of the G-L equations containing $J = (e/m)\ \rho_s v_s$ and $\Psi \sim (\rho_s/\rho)^{1/2}$ and gives $J_c = (e/m) \times (\rho_s v_s)_{max}$. The results of the calculation take on a simple analytic form in the limit $\Psi d/\lambda \ll 1$. In normalized form near T_c, Ginzburg gives

$$\frac{H_{ic}}{H_{cb}} = 0.544\frac{d}{\lambda}\left(1-\frac{H_e^2d^2}{H_{cb}^2 24\lambda^2}\right)^{3/2}, \tag{11}$$

where H_{ic} is the magnetic field produced by the critical current. Substituting the approximate temperature dependences for H_{cb} and λ Eqs. (6) and (7), the critical current density is

$$J_c(t) = 0.544\frac{c}{4\pi}\frac{H_{cb}(0)}{\lambda(0)}(1+t^2)^{1/2} \times\left[1-t^2-\frac{H_e^2d^2(1+t^2)}{H_{cb}^2(0)\lambda^2(0)24}\right]^{3/2}. \tag{12}$$

This equation is closely similar to the free-energy calculation and includes the additional dependence on the external magnetic field.

In summary we may state that the results of the various theoretical calculations are quite consistent. The temperature dependence of J_c is essentially the same in each calculation being governed by the $(1-t^2)^{3/2}$ term. The magnitude of J_c at $t=0$ is given by the free-energy calculation to be

$$J_c(0) = \frac{H_{cb}(0)}{2}\left(\frac{\sigma_n\Delta(0)}{\hbar}\right)^{1/2}. \tag{13}$$

For a typical film of tin this magnitude is between 2 and 3×10^7 A/cm^2. The more complicated calculations show that $J_c(0)$ should be approximately 70% of the above value.

B. Other Experiments

A series of experiments[10–13] on vacuum-deposited films were made using dc currents and compensating (cylindrical and disk-shaped) geometries. The re-

[3] E. A. Lynton, *Superconductivity* (Methuen and Company, Ltd., London, 1962), Chap. IV.
[4] J. Bardeen, L. N. Cooper, and J. R. Schrieffer, Phys. Rev. **108**, 1175 (1957).
[5] P. B. Miller, Phys. Rev. **113**, 1209 (1959).
[6] K. T. Rogers, Ph.D. thesis, University of Illinois, 1960 (unpublished).
[7] R. H. Parmenter, RCA Rev. XXIII, 323 (1962).
[8] V. L. Ginzburg and L. D. Landau, Zh. Eksperim. i Teor. Fiz. **20**, 1964 (1950).
[9] V. L. Ginzburg, Dokl. Akad. Nauk. (SSSR) **118**, 464 (1958) [English transl.: Soviet Phys.—Dokl. **3**, 102 (1958)].
[10] L. A. Feigin and A. I. Shal'nikov, Dokl. Akad. Nauk. (SSSR) **108**, 823 (1956) [English transl.: Soviet Phys.—Dokl. **1**, 377 (1956)].
[11] N. E. Alekseevski and M. N. Mikheeva, Zh. Eksperim. i Teor. Fiz. **31**, 951 (1956) [English transl.: Soviet Phys.—JETP **4**, 810 (1957)].
[12] N. I. Ginzburg and A. I. Shal'nikov, Zh. Eksperim. i Teor. Fiz. **37**, 399 (1959) [English transl.: Soviet Phys.—JETP **10**, 285 (1960)].
[13] N. E. Alekseevski and M. N. Mikheeva, Zh. Eksperim. i Teor. Fiz. **38**, 292 (1960) [English transl.: Soviet Phys.—JETP **11**, 211 (1960)].

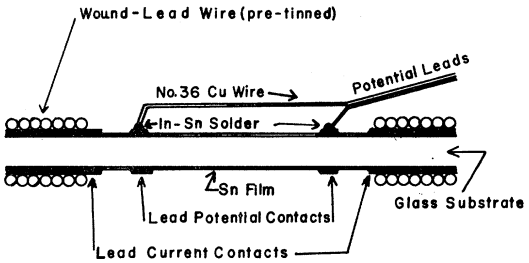

FIG. 1. Superconducting contacting arrangement for cylindrical samples.

sults were in poor agreement with theory, but at best[12,13] showed some accord with a $(1-t)^{3/2}$ dependence—the prediction of Ginzburg[9] very near T_c—for data within ≈ 0.2°K of T_c. Further work[14,15] involved the use of pulsed-current techniques to reduce the heating, but reverted to uncompensated planar films. Again no agreement with theory was found, but valuable information concerning the heating effects was obtained. Another pulse experiment was performed by Kolchin *et al.*,[16] in which the measurement was affected by the rise time of the current pulse. For fast rise times (≈ 0.1 μsec) the start of the resistive transition was displaced in the direction of lower currents. The authors assumed that this reduction was caused by eddy-current heating.

Mercereau and collaborators[17,18] have induced currents into ring-shaped films and by observing the trapped flux determined the critical current. They obtained a $(1-t)^{3/2}$ temperature dependence[17] for $(T_c-T)\leq 1.0$°K. Mercereau and Crane[18] found a peak in J_c near $t=0.65$. The magnitude of J_c at this temperature was $\approx 1.2\times 10^6$ A/cm^2 and decreased as the temperature was further reduced. For $t<0.5$, J_c was approximately constant at a value 0.9×10^6 A/cm^2.

By using a correction for the nonuniform current distribution in planar films of a few hundred Å, Glover and Coffey[19] have found both the magnitude and temperature dependence of the critical current over a substantial temperature range from a dc measurement. Their data are in good agreement with theory, but rely heavily on a mathematical expression for the variation of J across the film width.

In a cylindrical geometry, Hagedorn[20] has employed the fastest of today's pulse techniques with a 1-nsec pulse width and rise times of order 0.1 nsec. For a 1700-Å film forming part of the coaxial line, he measures the current necessary to produce 90% R_n. By applying an adiabatic correction to his data, he obtains a $(1-t^2)$ temperature dependence and claims a Silsbee[1] transition. Additional fast pulse measurements by Gittleman and Bozowski[21] show that there is a finite time associated with the first onset of resistance, depending on the fraction at which the current pulse exceeds i_c. Both investigations[20,21] place the intrinsic superconducting-to-normal switching times at less than 10^{-10} sec.

III. DESCRIPTION OF EXPERIMENT

A. Sample Fabrication and Mounting

The sample films of tin were prepared by vacuum deposition. The vacuum system employs two MCF60 oil diffusion pumps in series, each with a liquid-nitrogen cold trap. The evaporation chamber is all-metal and contains a liquid-helium cold trap. To deposit cylindrical films a rotating substrate and holder are inserted so that the substrate is in a slot cut in a metal block attached to the cold trap. A mask, with two $\frac{1}{16}$-in. openings 1 in. apart, may be rotated across the bottom of the block such that it just clears the rotating substrate. This allows for a preliminary deposition of rings of lead (Pb) to be used as current and potential contacts.

The substrates are usually hollow glass tubing, ≈ 2mm in outer diameter. A narrow capillary tube runs down the center of the glass tubing. Liquid nitrogen is continuously pumped through the capillary so that the depositions may be carried out with the substrate at 77°K. Modifications in this arrangement have been employed to utilize <1-mm-diam glass and solid sapphire single-crystal substrates. After bake-out, precooling and filling of the trap with liquid helium the tin evaporation is carried out at a constant pressure reading of $3\text{–}4\times 10^{-7}$ Torr. The actual pressure may even be lower than this.

Superconducting contacts are formed by winding a length of 0.3-mm Pb wire, pretinned with In-Sn eutectic solder, around each of the Pb current contacts. Soldering is then readily performed with In-Sn solder. The potential leads are of No. 36 copper wire and are attached to the narrow rings of deposited Pb film by a light drop of silver paint, or if superconducting potential contacts are desired, the copper wire may be directly soldered to the film with In-Sn solder. A diagram of the contacting arrangement is shown in Fig. 1.

There are two types of mounting for the sample depending on whether a dc or a pulse current measurement is to be made. A sketch of each type of mounting is given in Fig. 2. The principal difference in the two types of mounting is that the sample film forms the center conductor for the dc currents, while in the pulse currents the film is the outer conductor. This latter arrangement leaves the potential leads on the outer

[14] J. W. Bremer and V. L. Newhouse, Phys. Rev. **116**, 309 (1959).
[15] F. W. Schmidlin *et al.*, Solid State Electron., **1**, 323 (1960).
[16] A. M. Kolchin *et al.*, Zh. Eksperim. i Teor. Fiz. **40**, 1543 (1961) [English transl.: Soviet Phys.—JETP **13**, 1083 (1961)].
[17] J. E. Mercereau and T. K. Hunt, Phys. Rev. Letters **8**, 243 (1962).
[18] J. E. Mercereau and L. T. Crane, Phys. Rev. Letters **9**, 382 (1962).
[19] R. E. Glover and H. T. Coffey, Rev. Mod. Phys. **36**, 299 (1964).
[20] F. B. Hagedorn, Phys. Rev. Letters **12**, 322 (1964).
[21] J. I. Gittleman and S. Bozowski, Phys. Rev. **135**, A297 (1964).

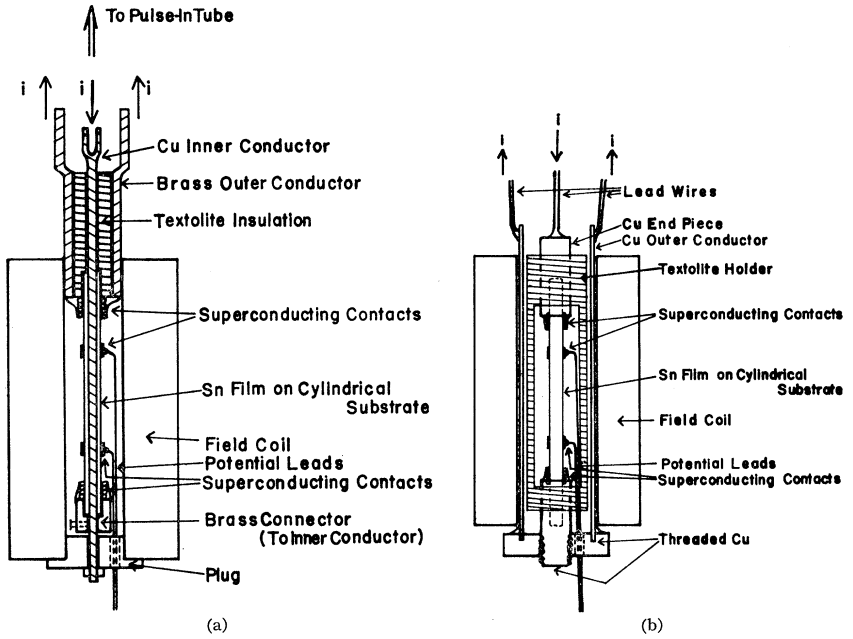

FIG. 2. Mounting of samples in cryostat, (a) for dc measurements and (b) for pulse measurements.

conductor in a region free of magnetic fields produced by the current, and thereby eliminates any inductive voltage pick-up which in other arrangements can be most troublesome. Note the coaxial symmetry for both fields and currents which ensures a uniform current flow everywhere in the film.

B. Dc Measurements

The cryostat is of standard design,[22] with the sample film in the liquid helium. The bath temperature is varied by pumping on the liquid helium and is stabilized by means of an automatic temperature controller.[22] Special high-current leads ($i>20$ A) into the cryostat were provided.

The dc circuit consists of a series of wire-wound rheostats and a multirange precision ammeter with a 6V automotive battery. The current can be plotted on the y axis of an x-y recorder. Using a dc microvolt amplifier, the potential across the sample is displayed on the x axis of the x-y recorder. This arrangement has a 10 μV full scale sensitivity on the lowest range.

The current is increased until a voltage appears on the x axis. A further increase will lead to Joule heating in the sample and a corresponding large increase in the voltage. Additional current transitions are recorded with various values of superposed magnetic field. Alternately the current through the sample can be set at different values up to the critical one, and the magnetic field transitions can be plotted.

The above procedure has been found to be applicable only near T_c ($T_c-T\approx 0.7$°K) because of the danger of film burn-out. In order to increase the temperature range, a stabilizing network is added, based on a design of Hilsch and Buckel.[23] A low-resistance Manganin wire is placed in parallel with the sample film. The resistance of the wire is made approximately 0.1% of R_n of the sample film. The sample film begins its superconducting-to-normal transition with the current all flowing through the film. As thermal runaway sets in, the current is shunted through the Manganin resistor. An additional microvoltmeter is connected across the shunt to determine the current through the shunt.

A typical x-y plot is shown in Fig. 3. It is important to develop a finite stable voltage across the sample so that the horizontal region can be extrapolated back to

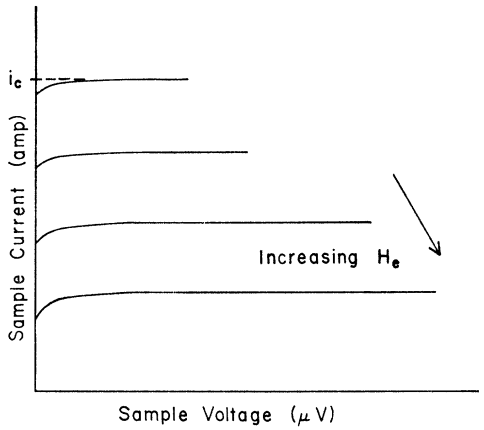

FIG. 3. Plot of current versus voltage for dc critical currents (schematic). Typical scales used: i_c: 0 to 3 A, V_s: 0 to 100μV.

[22] H. Meissner, Phys. Rev. **101**, 1660 (1956); *ibid.* **109**, 668 (1958).

[23] R. Hilsch and W. Buckel, *Proceedings of the Fifth International Conference on Low Temperature Physics* (University of Wisconsin Press, Madison, Wisconsin, 1958), p. 323.

TABLE I. General properties of tin films used in dc measurements.

Sample No.	Type	Diam (mm)	Average thickness (Å)	T_c (°K)	$H_c(0)$ (A/cm)	$J_c(0)$[a] (A/cm²)	Slope $1-t^2$ plot	Lowest t for stability	Average max. power for stab. (μ-W)
1	Glass	0.84	810	3.94	1220	4.0×10^6	1.52	0.69	38
2	Glass	0.85	780	3.84	1300	4.2×10^6	1.48	0.89	10
3	Sapp.	1.05	1100	3.88	800	7.5×10^6	1.49	0.86	77
4	Sapp.	1.00	720	3.87	1480	5.3×10^6	1.46	0.84	[b]
5	Sapp.	1.00	1720	3.86	490	8.2×10^6	1.52	0.92	120
6	Glass	1.70	810	3.86	1240	7.4×10^6	1.48	0.94[c]	30
7	Glass	1.65	670	3.86	1660	2.7×10^6	1.57	0.91	2
8	Glass	1.65	940	3.91	990	6.1×10^6	1.55	0.69	34

[a] $J_c(0)=i_c(0)/2\pi rd$.
[b] Potential leads opened during low-temperature measurements.
[c] Burnt out at $t=0.94$.

the ordinate. This horizontal region determines the critical current.

The above procedure is repeated at lower and lower temperatures until even with the shunt, the system becomes unstable. Here, the i_c measurements are stopped and low-current (100 μA) critical-field data are collected throughout the entire temperature range. These data, $H_c(t)$ versus t^2, are plotted to give the linear extrapolation to $H_c(0)$. By using the results of Blumberg,[24] for tin, of $H_c(0)$ as a function of thickness, the thickness of the cylindrical films may be found. Previous work at this laboratory[25] on planar tin films has carefully correlated the determination of thicknesses by multiple-beam interferometry with thicknesses from critical fields. Having found excellent agreement, we can expect reasonably accurate thicknesses from the $H_c(0)$ values since the planar and cylindrical films were vacuum-deposited in exactly the same manner. This alleviates the difficulties of performing interference measurements on cylindrical samples. Also to eliminate any effects of trapped flux within the ring formed by the film, i_c and H_c data were taken before and after the film was slit parallel to the cylinder axis. No difference was found in these measurements.

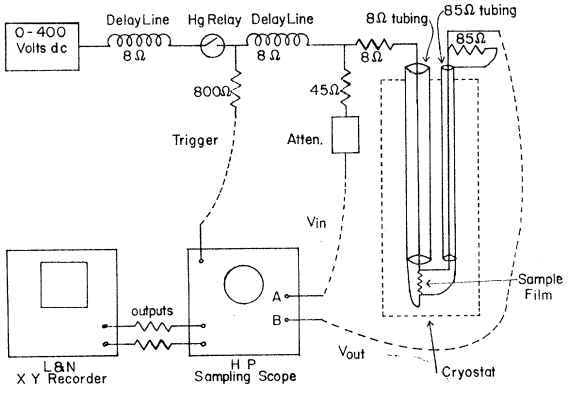

FIG. 4. Diagram of pulse current circuit. The delay lines are fabricated from 8-Ω coaxial cable.

[24] R. H. Blumberg, J. Appl. Phys. **33**, 1822 (1962).
[25] R. J. Duffy, Ph.D. thesis, Stevens Institute of Technology, 1964 (unpublished).

C. Pulse Measurements

A pulse system was designed to transmit fast rise time, high-current pulses to a sample film mounted in the cryostat. Figure 4 gives a schematic diagram of the pulse system. The characteristic impedance of the line has been chosen to be 8 Ω. When the line is simply terminated in an 8-Ω matching resistor the pulse is flat and has rise times less than 1 nsec. The 8-Ω matching resistor had to be placed outside the cryostat. Then a specially designed thin-walled coaxial tube of characteristic impedance just over 8 Ω goes into the cryostat to the sample. With this type of arrangement an inductive peak appears on the leading edge of the input voltage pulse. The current shows a corresponding reduction which can be verified with a normal conducting sample.

The voltage appearing at the input end of the 8-Ω matching resistor, V_{in}, is fed into channel A of a dual beam HP 185A sampling oscilloscope. A second thin-walled coaxial tube with 85-Ω characteristic impedance goes into the cryostat and is connected to parallel leads coming from the potential contacts of the sample. This coaxial tube is terminated in an 85-Ω matching resistor and the voltage across this resistor, V_{out}, is fed into channel B of the sampling oscilloscope. V_{out} is zero when the sample is fully superconducting.

An important feature of this oscilloscope is a manual scan with outputs so that V_{out} versus V_{in} for fixed time can be plotted on the x-y recorder. These V_{out} versus V_{in} curves determine the critical current. Since only the flat portions of the pulse are of interest, simple circuit analysis can be used to relate V_{in} to the current i. To a good approximation this is just $i=V_{in}/(8\,\Omega)$, since the 8-Ω matching resistor is much larger than the normal resistance of the sample film (usually a few tenths of an ohm).

In addition to the x-y plots, the various voltage traces as a function of time are photographed. Furthermore,

as in the dc measurements, the external magnetic field can be applied and current-field data obtained. A characteristic V_{out} versus V_{in} plot is shown in Fig. 5.

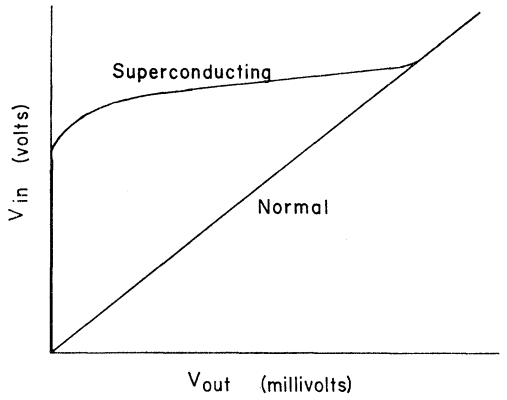

FIG. 5. Plot of V_{out} versus V_{in} for pulsed critical currents (schematic). Typical scales are: V_{out}: 0 to 1 V, V_{in}: 0 to 50 V.

IV. Dc EXPERIMENTAL RESULTS

A. Critical-Current Data

Eight cylindrical samples were successfully fabricated and measured. The salient properties of these samples are listed in Table I. The substrates were glass or sapphire ranging in diameter from 0.84 to 1.70 mm. The films had average thicknesses from 670 to 1720 Å as determined by the $H_c(0)$ intercept. The critical current as measured by dc currents is defined as the first onset of a normal voltage along the film. The resistance, thus developed, is $\approx 10^{-3}R_n$. Measurements for which it was impossible to obtain a stable voltage are discarded. This limits the temperature range over which i_c can be measured.

The data for i_c, as defined above, are plotted on a log i_c versus $\log(1-t^2)$ scale. The slope gives the power of $1-t^2$, while the intercept at $t=0$ gives $i_c(0)$. Table I lists $J_c(0)$ and the power of $1-t^2$ for each of the samples. $J_c(0)$ is equal to $i_c(0)/2\pi rd$, where r is the radius of the substrate and d the average film thickness. Also tabulated are the lowest reduced temperature at which a stable voltage could be obtained and the average maximum power (i_cV_s) for which the sample film remains stable.

Figure 6 is a plot of i_c versus $1-t^2$ for sample 8 (940 Å). This sample was measured three times within five days which accounts for the large number of data points. The slope of the line is 1.55 and $i_c(0)$ is 29A corresponding to a $J_c(0)=6.1\times10^6$ A/cm². The other samples had similar plots, the important parameters of which are presented in Table I.

B. Current Data with External Field

In these measurements, i_c is also defined as the first onset of voltage while now an external magnetic field is applied. Typical curves for these data are shown in Fig. 7 for sample 8. A log i_c versus H_e plot is used with the reduced temperature as a parameter. A family of curves, almost parallel, is obtained which start out essentially horizontal in zero field, decreasing with increasing field to nearly a vertical slope close to the maximum field (H_c at that temperature). All eight samples give plots similar in shape differing only, as expected, in magnitudes.

C. Discussion

By reviewing the results of Table I, a number of assertions can be made concerning the dc critical current measurements. The power of $1-t^2$ is close to 1.5 for all eight of the samples. The average value of 1.51 can be compared to the theoretical predictions in Sec. IIA. For our range of temperatures, the dominant term of the temperature dependence is $(1-t^2)^{3/2}$. Therefore, the experiment and the theory are in excellent agreement. This would confirm our criterion for measurement and our definition of i_c as a first onset.

Recall that the magnitude of $J_c(0)$ as given by Eq. (13) was estimated at between 2 and 3×10^7 A/cm² for films in our range of thickness. The more complicated calculations reduce the magnitude to 1 to 2×10^7 A/cm². The experimental data for the eight samples are all lower by about a factor of 2.

$J_c(0)$ is found by dividing $i_c(0)$ by the cross-sectional area of the film ($2\pi rd$). It would seem that the main uncertainty in the expression for $J_c(0)$ appears in the value of d. The film will always have some variations in thickness and "weak" spots. For a uniform current distribution these regions would be expected to support a lower supercurrent density than their surroundings.

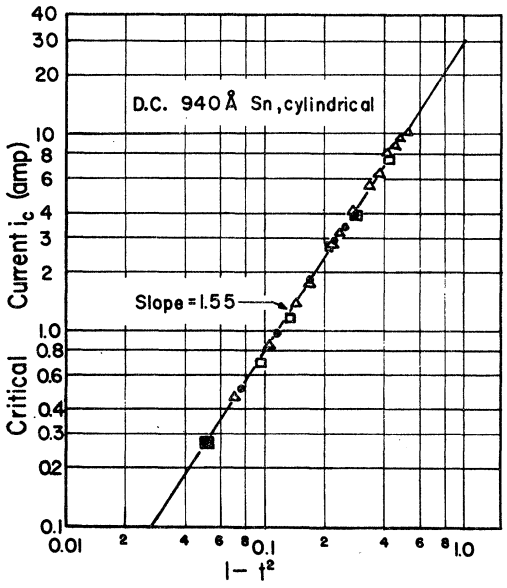

FIG. 6. Temperature dependence of the critical current for sample 8, 940 Å.

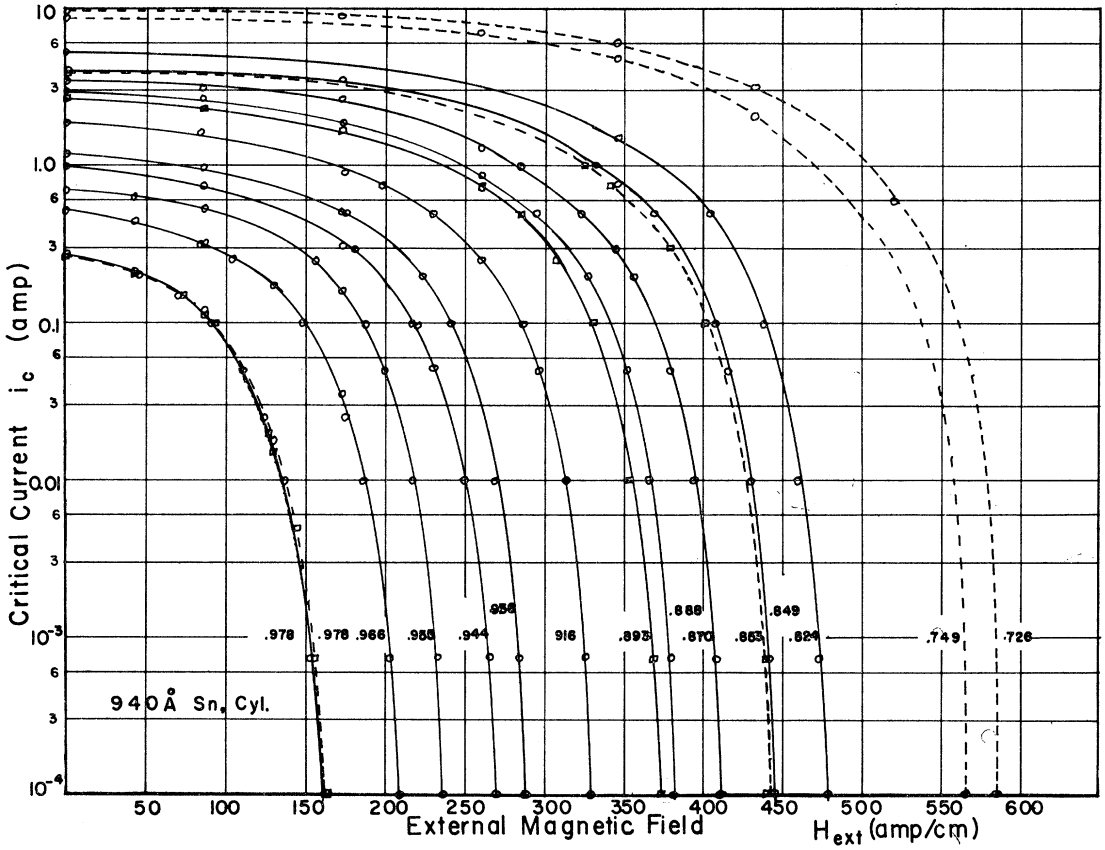

FIG. 7. Critical current versus superposed magnetic field with reduced temperature as a parameter for sample 8, 940 Å.

Note that it is the current density and not the current which destroys the superconductivity. And since the critical current measurement is of a first onset type it will be these regions which will first become normal conducting. Therefore, in the calculation of $J_c(0)$, d should be replaced by a smaller effective thickness. In order to estimate the magnitude of the effective thickness, we can examine the critical-field transitions of the films. There is a "tailing" of the critical field to higher values just before the full R_n is reached. The value of the maximum H_c will be related to the thickness of the thinnest regions. The H_c data show the thickness variations to be less than 100 Å. Thus, the effective thickness will only partially account for the deviations with theory in the magnitude of $J_c(0)$.

In type-II bulk superconductors the measured J_c's are always less than the predicted ones.[26] In this case degradation effects due to the Lorentz force are responsible for the reduced values of J_c. The Lorentz force in films could also cause a resistance to be measured at a lower value of current. For the present case, only the current-produced magnetic field can interact with the current to produce the Lorentz force. In none of the existing theories for films are these effects taken into account.

[26] Y. B. Kim *et al.*, Rev. Mod. Phys. **36**, 43 (1964).

In practical units (i_c in amperes, H in A/cm, and lengths in cm), the Ginzburg[9] equation [Eq. (12)] becomes

$$i_c(t)=0.544(2\pi r)H_{cb}(0)(1+t^2)^{1/2} \times\frac{d}{\lambda(0)}\left[1-t^2-\frac{H_e^2d^2(1+t^2)}{H_{cb}^2(0)\lambda^2(0)24}\right]^{3/2}. \quad (14)$$

For $i_c\rightarrow 0$ and $H_e=H_c$ this equation reduces to the usual G-L critical field equation for the thin film limit. By substituting the experimental values of H_c and the known value[27] of $H_{cb}(0)=242$ A/cm, the ratio $d/\lambda(0)$ can be found. With this ratio the full Eq. (14) can be used for comparison with the current-field data. However, in the limit of $H_e=0$, Eq. (14) reduces to an i_c versus t equation and gives an i_c larger by a factor of 2 than the experimental data. Thus, if we simply use Eq. (14) with the parameter $d/\lambda(0)$, we will obtain a family of curves at different temperatures which are in agreement with the experimental data at low currents, but deviate at the larger currents for nearly zero field. In order to examine the functional dependence of Eq. (14) with the current-field data, we adjust the constant

[27] J. M. Lock, A. B. Pippard, and D. Schoenberg, Proc. Cambridge Phil. Soc. **47**, 811 (1951).

TABLE II. General properties of cylindrical films used in pulsed measurements.

Sample No.	Type	Diam (mm)	Supercond. contacts	Average thickness (Å)	T_c (°K)	$H_c(0)$ (A/cm)	$J_c(0)$[a] (A/cm²)	Initial slope of $1-i^2$ plot	t of break
9	Glass	3.1	No	820	3.90	1200	8.2×10^6	1.46	0.93
10	Glass	3.1	No	740	3.85	1395	7.3×10^6	1.43	0.94
11	Glass	3.0	Yes	910	3.88	1040	8.3×10^6	1.40	0.94

[a] $J_c(0)=i_c(0)/2\pi rd$.

at the front of this equation such that the magnitudes of i_c for $H_e=0$ agree with the data. Only one new constant is needed for all temperatures since the data do follow the temperature dependence given by the equation.

Let us carry out this procedure on sample 8. For the limit $i_c\rightarrow 0$, Eq. (14) gives $d/\lambda(0)=1.07$ which is constant to within a few percent in the temperature range of interest. Next the constant 0.544 is adjusted to 0.163 such that it gives the proper magnitude of i_c for $H_e=0$. Substituting this single new constant, $H_{cb}(0)$, and $d/\lambda(0)$ into Eq. (14), i_c may be found at any temperature. This equation was programmed for the 1620 computer at the Stevens Computer Center and the theoretical curves obtained. A comparison between the experimental data and this Ginzburg theory is given in Fig. 8 where the solid lines are the theoretical curves while the ×'s represent the experimental data. Note that the experimental points are slightly below the theoretical curves. This can arise from variations in film thickness, causing different portions of the film to become normal for i_c large and i_c small.

V. PULSE EXPERIMENT

A. Critical Current Data

Three cylindrical samples were fabricated and pulsed-current data were taken. The noteworthy properties of the cylindrical samples are listed in Table II. In these measurements the critical-current transition is completely traversed from the first onset to the full normal state. This leaves the definition of i_c somewhat arbitrary. The first-onset definition is used and compared with the dc measurements, then the critical currents necessary to force higher percentages of R_n are studied.

Again we can use the $\log i_c$ versus $\log(1-t^2)$ plot to examine the data. Now there will be a group of critical currents for each temperature, the lowest being the first onset i_c, the others higher percentages of R_n (usually 10, 25, 50, 75, and 90%). Such a plot is given in Fig. 9 for sample 9, 820 Å. By following the first onset data a slope of 1.46 is generated until a break occurs at $t=0.93$, then the data points follow a lower slope of about 0.5. The temperature at which this break takes place is rather high when compared with the temperature ranges of the dc measurements. The other definitions of i_c lead to lower slopes as the percentage of R_n is increased in the region of $t>0.93$, but these also break away from their initial straight lines below $t=0.93$.

There are two ways to resolve $i_c(0)$ and $J_c(0)$. The first is to extrapolate the low-temperature data to absolute zero. This gives, for the first onset data, $i_c(0)=10$A corresponding to $J_c(0)=1.25\times10^6$ A/cm². Or, the initial high-slope region can be extrapolated to $t=0$. This intercept gives, for the first onset data, $i_c(0)=65$A and $J_c(0)=8.2\times10^6$ A/cm². In Table II we collect the data from the latter interpretation since these data are more easily compared with the dc measurements.

The remaining two cylindrical samples have i_c plots remarkably similar to each other and to the previous sample (see Fig. 9). The pertinent parameters are listed in Table II.

B. The Critical Current Transition

A multiexposure oscilloscope photograph can be taken first with the current pulse below the critical

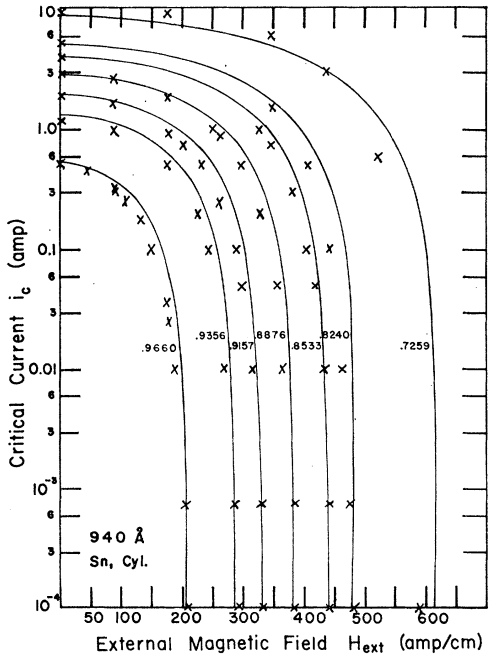

FIG. 8. Theoretical curves and experimental data of i_c versus H_e with reduced temperature as parameter for sample 8, 940 Å.

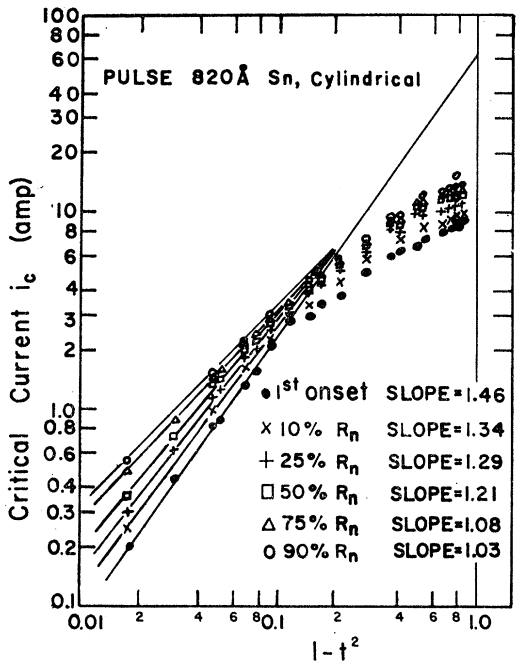

FIG. 9. Temperature dependence of the pulsed-critical current for sample 9, 820 Å.

value so that only a V_{in} pulse will appear, and then for successively higher values of current where now V_{out} traces form. In this manner, various levels of the transition are viewed. A typical photograph is shown in Fig. 10.

In this figure the smallest V_{in} pulse (the first pulse to rise; with the overshoot on its leading edge) produces no V_{out} pulse (the lowest horizontal line)—the tin film is superconducting. After an increase in current the corresponding V_{in} pulse now produces a slowly rising V_{out}. The procedure is repeated with higher and higher currents each giving a faster rising V_{out} pulse and restoring larger fractions of the normal resistance. The largest V_{in} pulse is really a superposition of two traces each producing a different V_{out} pulse (the top two traces). This is accomplished by turning on the external magnetic field to drive the sample fully normal and then "hitting" it with the current pulse (see top-most trace in Fig. 10). Note that for this V_{in}, the current alone is still too small to drive the sample fully normal.

Similar photographs were taken throughout the temperature range and some of these are given in Fig. 11. A number of salient characteristics of the current transition are illustrated in these traces. One of these is the delay time associated with the inception of the V_{out} pulse. Defining i_c as the current which produces the first onset of voltage across the film at the 50-nsec time point, we find long delay times for i just above i_c. As the current is increased to higher values the delay times become shorter. All delays are measured with respect to the V_{out} pulse when the sample is normal conducting. By plotting the delay time τ_d against $(i/i_c)-1$, a series of data points is obtained as depicted in Fig. 12.

A most important characteristic illustrated in the photographs is the shape of the V_{out} pulse after the delay. The pulse does indeed become flat at values corresponding to a resistance less than R_n. If heating were affecting the sample its resistance would continually rise towards the full normal value and thus the V_{out} pulse would never become flat at a fraction of R_n.

C. Current Data with External Field

The pulsed critical current transitions are also measured in the presence of an applied magnetic field. The method is similar to that used in the dc measurements whereby various currents are "fed" into the sample film and the critical field transition is recorded for each value of current. Choosing the first onset definition of i_c, the data are plotted as log i_c versus H_e with temperature as the parameter. This plot is shown in Fig. 13 for sample 9.

Near T_c, the same general curve shape as in the dc data appears with an almost parallel family of curves. However, for lower temperatures the curves start out in the low-current region with this parallel quality, but soon lose it as higher currents are reached, and for very high currents (H_e nearly zero) the curves tightly "squeeze" together. The temperature at which this depression first occurs is connected with the temperature of the break in the i_c versus $(1-t^2)$ plot: $t=0.93$. Above $t=0.93$ the family of curves is essentially parallel,

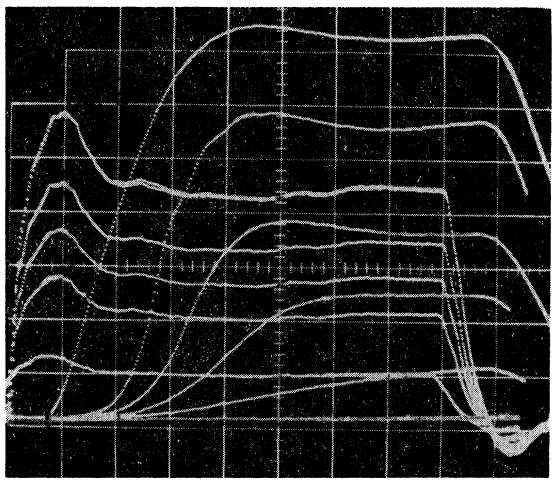

FIG. 10. Input (V_{in}) and output (V_{out}) pulses versus time for sample 10 at $t=0.977$. Time scale: 10 nsec/cm. The input voltages show an overshoot caused by the 8-Ω line into the cryostat. The corresponding lowering of the rise time of the current can be seen in the uppermost output pulse, where the sample was normal. V_{in} scale was 3.8 V/cm which gives a current of 0.53 A/cm, while the V_{out} scale was 0.1 V/cm. The lowest horizontal output curve goes with the lowest input pulse, etc., until the two highest ones which have the same V_{in}. Here the V_{out} pulse was taken with and without a superimposed magnetic field. Note the delay times in V_{out}.

but below the "squeezing" starts and becomes especially severe at the lowest temperatures.

D. Discussion

The $\log i_c$ versus $\log(1-t^2)$ plots exhibit a distinct behavior in each of two regions. Very near T_c the data are linear for all percentages of R_n with the first onset points giving an average slope of 1.43. This could be claimed as fair agreement with the theoretical prediction of 1.50, which was closely verified by the dc measurements. For higher percentages of restored resistance, the slopes become less, eventually reaching a value near 1.0 for 90% resistance. This is the temperature dependence predicted from the Silsbee hypothesis.[1] It should also be recalled that the very fast pulse measurements of Hagedorn,[20] when corrected for the adiabatic[28] superconducting-to-normal transition, give a $1-t^2$ temperature dependence for 90% of R_n.

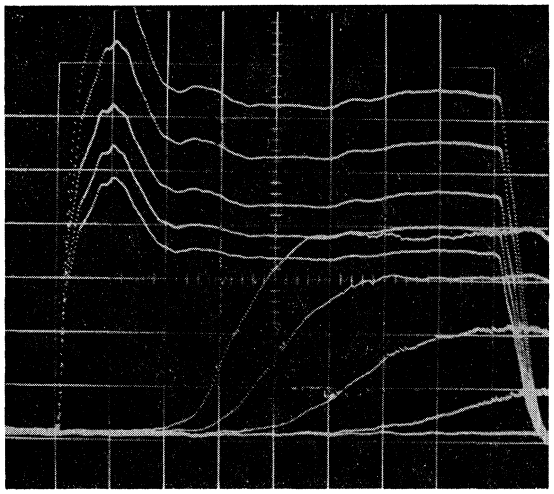

(a)

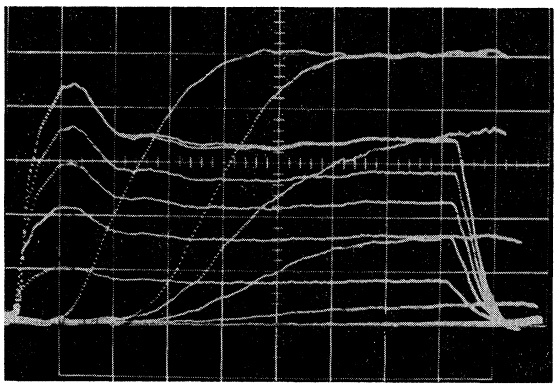

(b)

FIG. 11. Input and output pulses for: (a) Sample 11, $t=0.858$; $V_{in}=12.2$ V/cm, $V_{out}=1.0$ V/cm. (b) Sample 10, $t=0.733$; $V_{in}=38.1$ V/cm, $V_{out}=1.0$ V/cm. The time scale is in both cases 10 nsec/cm. The input and output pulses can be identified as indicated in Fig. 10. Only in (b) was there a magnetic field superimposed as in Fig. 10.

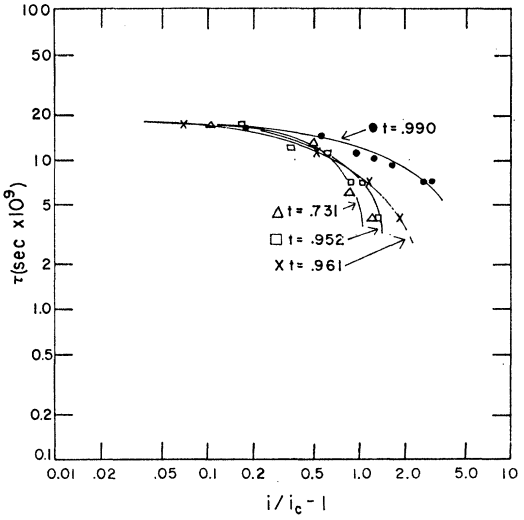

(a)

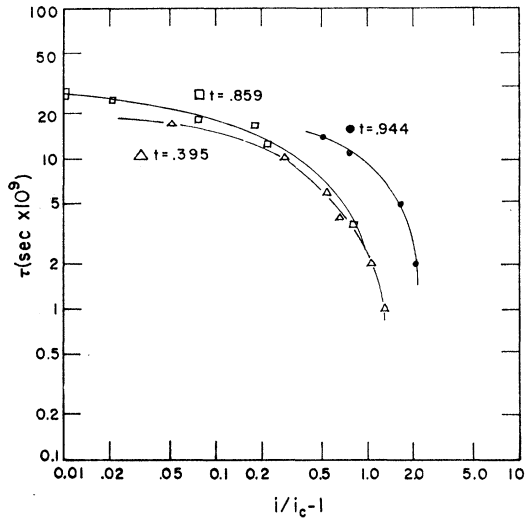

(b)

FIG. 12. Plot of delay time versus $(i/i_c)-1$ with reduced temperature as a parameter. (a) Sample 10; (b) sample 11.

At $T<0.93T_c$ the slopes for all percentages of R_n are reduced to essentially the same slope of about 0.5. Attempts to account for the deviations using the usual Joule heating arguments meet with difficulties. In the first place, the use of 80-nsec pulses at a repetition rate of 120 pulses/sec has reduced the average power input by a factor of 10^{-5} over the dc current method. Yet the deviations start at a comparatively higher temperature

[28] Since our effective pulse lengths are some 50 times greater than the short duration pulses used by Hagedorn, we would not expect the adiabatic correction to apply to our data. However, we did apply this correction to our data and found it only reduces the slopes, making the curves completely nonlinear, and thus confirmed our expectation.

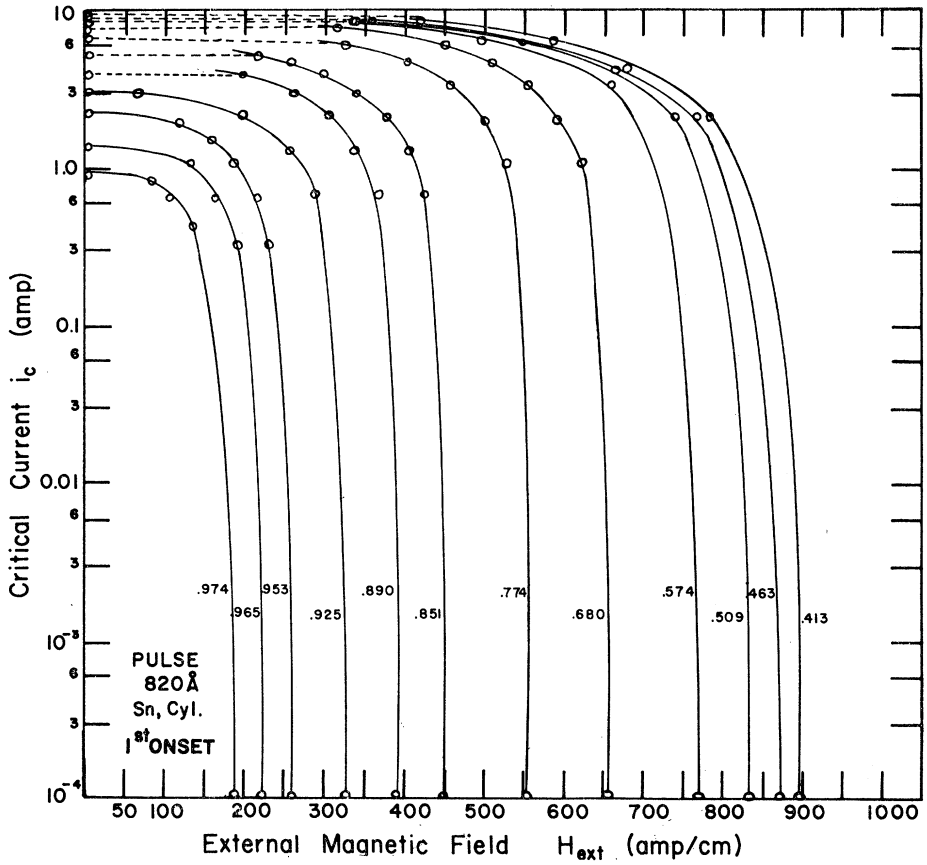

FIG. 13. Pulsed critical currents versus superposed magnetic field with reduced temperature as parameter. Sample 9, 820 Å.

well within the range of stable dc measurements. Also, as mentioned before, the photographs of the transitions show the V_{out} pulse to become flat with the full current flowing through the sample film. Heating effects once started would tend to reinforce and propagate along the entire film length while the current is constant. These observations indicate that two regions must be considered in any explanation of the transition by heating. There is an initial region characterized by a delay time of 10–30 nsec. Here heating could aid the normal regions in spreading across the film thickness, but there could not be much propagation along the film in so short a time. During the second phase, which appears as a flat V_{out} pulse on our time scale heat can propagate[14] with a small velocity along the film proper. Our photographs show that we are free of this latter type of propagation. But most important, there is no explanation for the *first onset* of the normal state by heating at such low currents since there are practically no sources of heat anywhere near or in the tin film.

Another possibility of heating, as suggested by Kolchin *et al.*,[16] is that arising from eddy currents. Yet due to the thinness of the films and the use of superconducting contacts, the heating power of eddy currents is rendered negligible. Also the possibility of the induced currents exceeding the critical current can be excluded on the basis of the small magnetic flux available with the thin films in a cylindrical geometry.

The strange behavior of the temperature dependence below $t=0.93$ is reflected in the magnitudes of J_c. By following the experimental data to absolute zero, values of $J_c(0)$ between 1 and 2×10^6 A/cm^2 are found for the three samples, using the first onset definition. These values are $\frac{1}{3}$ to $\frac{1}{6}$ of the dc measured values and about an order of magnitude below the theoretical values. By extrapolating the linear regions above $t=0.93$ to absolute zero, current densities in close agreement with the dc $J_c(0)$ are obtained. The $J_c(0)$ values thus obtained are 7 to 8×10^6 A/cm^2, about $\frac{1}{2}$ of the theoretical calculations.

No other experiments using a fast pulse technique have given consistent results. The microwave critical-current technique of Sherrill and Rose[29] gives deviations from theory which are similar to the present work. Also Flippen[30] reports that the critical field is greatly reduced when a fast-pulsed magnetic field is used. This backlog of experimental data being compatible with the present work, there is substantial evidence for an unaccountable

[29] M. B. Sherill and K. Rose, Rev. Mod. Phys. **36**, 312 (1964).
[30] R. B. Flippen, Phys. Rev. **137**, A1822 (1965).

resistance effect due to rapidly changing currents and fields in superconductors. Furthermore, since the usual heat and heat propagation arguments are ineffective, the indication is that this effect is fundamental and is related to the short rise times of the current pulses producing a very large dJ/dt.

Most recently, Anderson, Werthamer, and Luttinger[31] have given a phenomenological derivation of the "extra" time-dependent Ginzburg-Landau equation. This, they claim, can give rise to a resistance in a superconductor in association with a time dependence of Ψ. The introduction into the theory of $d\Psi/dt$ from the acceleration of a current could well account for the lowered values of i_c that we have found with the pulse technique.

Photographs of the critical current transition besides giving information as to the lack of heating also reveal delay times in the nanosecond range which are an indication of the superconducting-to-normal switching time. The delay times have been previously discussed by Gittleman and Bozowski.[21] By comparing their data with our Fig. 12, we note a similar pattern of the data, but with our delay times somewhat longer. In addition, we find much longer delay times for $t>0.93$, which also are temperature-dependent, than below where the delay times are essentially independent of temperature.

The pulsed-current-field data can again be compared to Ginzburg's[9] calculation, Eq. (14). Now, however, it is obvious that at the lower temperatures ($t<0.93$) the experimental data deviate widely from theory.

VI. CONCLUSIONS

The dc experiment, utilizing a cylindrical geometry, gives an unambiguous method for determining the critical current. The temperature dependence is in excellent agreement with theory. Also the critical-current densities obtained when we simply divide i_c by the cross-sectional area of the film are higher and closer to theory than other reported uncorrected values. The current-field measurements are the first such measurements performed on tin films. These data give a family of curves closely resembling those of Ginzburg's calculation when adjusted in magnitude.

The pulse data for $t>0.93$ are in fair agreement with theory and the dc data. Below this temperature the results are extensively different. The deviation is attributed to the large values of dJ/dt which give rise to dissipative effects.

ACKNOWLEDGMENTS

The authors wish to thank Professor W. Bostick for making departmental funds available for this research. The helium gas was obtained, free of charge, from the U. S. Office of Naval Research, which also supplied instruments on an equipment loan contract. Several large pieces of equipment were purchased with funds from the Charles and Rosanna Batchelor Memorial Foundation. We are grateful to H. Gould for programming of the computer and G. Wirth for the operation of the helium liquefier.

APPENDIX: CRITICAL CURRENTS IN PLANAR TIN FILMS

A. Extension of the Theory to the Planar Geometry

Although the theories of critical currents remain the same for a nonuniform current distribution, the current density J is a function of position in the film. $J(x)$ is small at the center, but increases rapidly towards the edges (x is measured from the center of the film to the edges). In a first-onset measurement, it will be in the edges, where J is large, that the normal state will first appear and we must relate this edge-current density to the total current. Since our films were not very thin ($d>\lambda$), we are unable to use the analytic expression for $J(x)$ as given by Rhoderick and Wilson[32] and successfully applied in the experiments of Glover and Coffey.[19]

Unfortunately, for our requirement of $d>\lambda$ there is no analytic expression of $J(x)$. Marcus[33] has calculated an expression for $d>\lambda$ which relates the current density in the edges to that at the center:

$$J(w/2)=J(0)[wd]^{1/2}/1.65\lambda; \qquad \text{(A1)}$$

w is the film width. In order to relate the current flowing

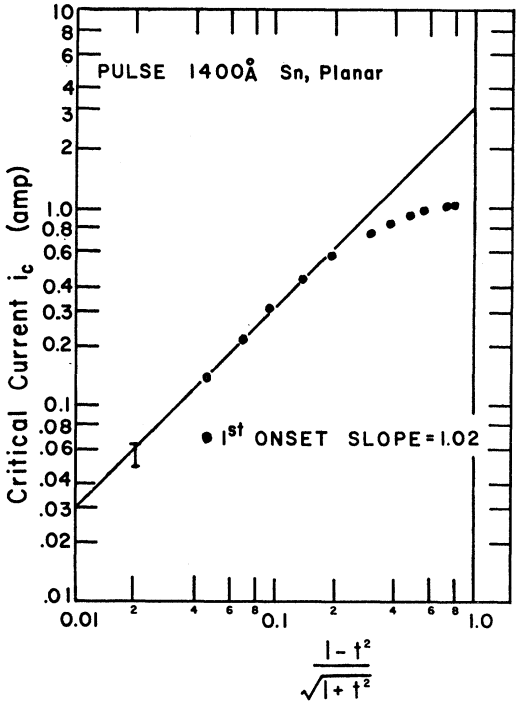

FIG. 14. Temperature dependence of the pulsed-critical current for the planar sample 14, 1400 Å.

[31] P. W. Anderson, N. R. Werthamer, and J. M. Luttinger, Phys. Rev. 138, A1157 (1965).

[32] E. H. Rhoderick and E. M. Wilson, Nature 194, 1167 (1962).

[33] P. M. Marcus (unpublished).

TABLE III. General properties of planar films used in pulsed measurements.

Sample No.	Width (mm)	Average thickness (Å)	T_c (°K)	Initial slope of $(1-t^2)/(1+t^2)^{1/2}$ plot	Measured J_{co}[a] (A/cm²)	Theoretical J_{co}[b] (A/cm²)	t of break
12	0.25	2600	3.92	1.00	3.5×10^7	4.25×10^7	0.82
13	0.25	1950	3.87	1.00	3.7×10^7	4.4×10^7	<0.9[c]
14	0.57	1400	3.84	1.02	7.6×10^7	6.0×10^7	0.85

[a] Corrected for edge build-up [see Eq. (A4)].
[b] See Eq. (13).
[c] No data below $t=0.9$ because of sample burnout while using dc currents.

through the film i to $J(0)$, we employ the following approximation

$$i=KwdJ(0), \tag{A2}$$

where K is a constant to be estimated. If we had an analytic function for $J(x)$, we could then integrate over x and obtain an exact number for K. This is done in the thin film case of Glover and Coffey and gives K the value of $\pi/2=1.57$. As the film thickness increases so will $J(x)$ build up in the edges. Since our films are from three to four times thicker than those used by Glover and Coffey, we estimate the value of K at 3. Then we can relate i to the edge-current density where the first onset of normal resistance will occur, by substituting Eq. (A1), obtaining

$$J(w/2)=i/[4.95\lambda(wd)^{1/2}]. \tag{A3}$$

Thus the magnitude of the critical-current density at absolute zero becomes

$$J_{co}=i_c(0)/[4.95\lambda(0)(wd)^{1/2}]. \tag{A4}$$

For the temperature dependence of i_c, we divide J_c by J_{co} noting that the critical-current density does not have its temperature dependence affected by the edge build-up—it remains the same at the $(1-t^2)^{3/2}$ approximation. Therefore

$$\frac{J_c}{J_{co}}=\frac{i_c(t)/\lambda(t)}{i_c(0)/\lambda(0)}=(1-t^2)^{3/2}. \tag{A5}$$

Substituting Eq. (7), we have for the temperature dependence

$$i_c(t)/i_c(0)=(1-t^2)/(1+t^2)^{1/2}. \tag{A6}$$

B. Pulsed-Current Measurements in Planar Films

The pulse method used to determine i_c in the planar films is similar to that employed in the cylindrical samples. The general properties of the planar films are given in Table III.

The first-onset critical current data are now plotted as $\log i_c$ versus $\log[(1-t^2)/(1+t^2)^{1/2}]$. Such a plot is shown in Fig. 14 for sample 14. The data near T_c lie along a straight line with slope 1.02. As the temperature becomes lower ($t<0.85$), there is a drifting of the points away from the line. This deviation towards lower currents is similar to that found previously in the pulsed-current measurements of cylindrical films. Since the deviation cannot readily be explained, we will base our analysis on the linear portion. The slope of ≈1.0 does obey the theoretical temperature dependence. The two other planar films have slopes of exactly 1.0 for temperatures close to T_c and exhibit the same deviations below a "break" temperature. These salient quantities are listed for each sample in Table III.

If the linear region is extrapolated to absolute zero $i_c(0)$ is determined. Substituting this $i_c(0)$ into Eq. (A4) [$\lambda(0)$ is determined by Tinkham's[34] model], a value of 7.6×10^7 A/cm² is calculated. Then by using the experimental value of σ_n[35] and the properties of bulk tin, J_{co} can be computed from Eq. (13). The result is $J_{co}=6.0\times10^7$ A/cm². Better agreement is found for the other samples as can be seen in Table III. Even if the 70% correction of the more refined calculations for J_{co} is used, the good agreement is maintained.

[34] M. Tinkham, Phys. Rev. **110**, 26 (1958).
[35] σ_n is found to be much larger in these thick planar films than in the rather thin cylindrical samples.

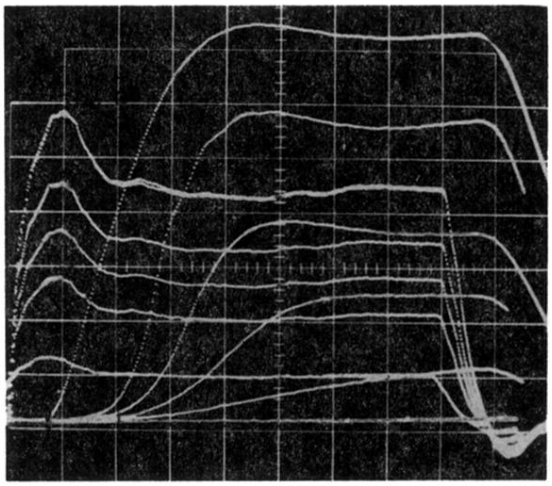

FIG. 10. Input (V_{in}) and output (V_{out}) pulses versus time for sample 10 at $t=0.977$. Time scale: 10 nsec/cm. The input voltages show an overshoot caused by the 8-Ω line into the cryostat. The corresponding lowering of the rise time of the current can be seen in the uppermost output pulse, where the sample was normal. V_{in} scale was 3.8 V/cm which gives a current of 0.53 A/cm, while the V_{out} scale was 0.1 V/cm. The lowest horizontal output curve goes with the lowest input pulse, etc., until the two highest ones which have the same V_{in}. Here the V_{out} pulse was taken with and without a superimposed magnetic field. Note the delay times in V_{out}.

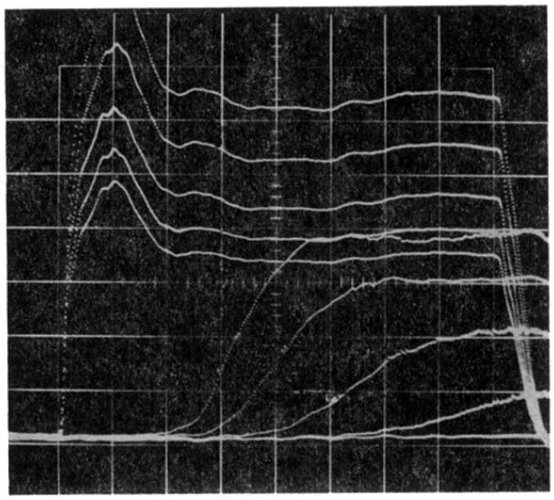

(a)

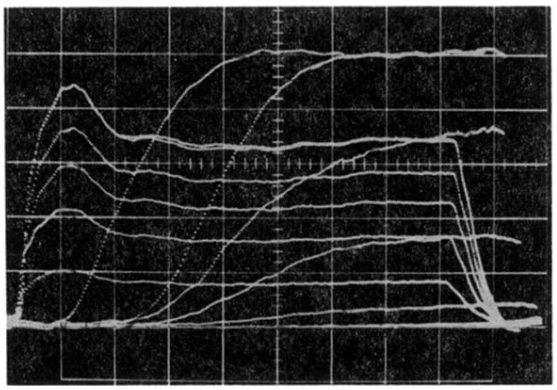

(b)

FIG. 11. Input and output pulses for: (a) Sample 11, $t=0.858$; $V_{in}=12.2$ V/cm, $V_{out}=1.0$ V/cm. (b) Sample 10, $t=0.733$; $V_{in}=38.1$ V/cm, $V_{out}=1.0$ V/cm. The time scale is in both cases 10 nsec/cm. The input and output pulses can be identified as indicated in Fig. 10. Only in (b) was there a magnetic field superimposed as in Fig. 10.